Optimum Parameters of Kelvin-defined Dampers Connecting Symmetrical Three-adjacent-structure System

Yushuang Guan*, Hongyu Li[a], Huangsheng Sun[b]

College of Civil Engineering and Architecture, Shandong University of Science and Technology, Qingdao, Shandong, 266590, China

*2928614903@qq.com, [a]2710683484@qq.com, [b]shs7528@sdust.edu.cn

Abstract. Based on the simplified model of symmetrical three adjacent structures interconnected by Kelvin-modeled dampers, the influences of connecting parameters, i.e., stiffness and damping, on the structural seismic responses are investigated numerically. Taking the structural vibration energy as the optimization criterion, the optimum stiffness and damping parameters of the connecting damper as well as the corresponding structural seismic reduction factors (SRFs) are obtained for the three control criteria, respectively. Then the effects of structural frequency-ratio, mass-ratio, on the optimum connecting parameters and the corresponding SRFs are analyzed. In addition, the applicability of the optimum connecting parameters for an example of MDOF-modeled adjacent structures group is verified by comparing the optimal linking parameter values and SRF of the example with those of the simplified model. Finally, time history analysis on the controlled structures under earthquake excitation is conducted and the reduction effectiveness in terms of displacement, interlayer shear force and vibration energy are analyzed. The results show that the optimum connecting parameters are related to the structures frequency-ratio and mass-ratio. The increase in structures natural vibration frequency difference would improve the reduction effectiveness. The optimum parameters for the control criteria are not equal and the structures could not obtain the best control effectiveness simultaneously. The proposed optimal connecting parameters derived from simplified model are applicable for MDOF system with the SRF increases by less than 0.051.

Keywords: three adjacent structures; seismic mitigation; connecting parameter; parameter optimization; seismic reduction factor.

1 Introduction

Adjacent buildings are often constructed very close to each other to meet the increasing demand for construction in densely populated urban centers while urban land is limited. In addition, there are many cases when a large building is divided horizontally into many smaller pieces by expansion or seismic joints and then adjacent structures take

F. Ding et al. (eds.), *Proceedings of the 2024 International Conference on Civil Engineering Structures and Concrete Materials (CESCM 2024)*, Advances in Engineering Research 247,
https://doi.org/10.2991/978-94-6463-564-5_14

shape. For instance, a building composed of towers and podiums with different heights is frequently separated into several parts by leaving gaps between them to prevent cracks caused by differential settlement of foundations, or to reduce earthquake-induced load effects in seismic regions. More often than not, adjacent structures may have different dynamic properties since they are of different heights, mass and stiffness vertical distributions. The collision phenomenon may occur between such adjacent structures during the strong earthquakes when the space between them is not sufficient [1-3]. A number of studies have revealed that connecting the adjacent structures together with passive energy dissipation devices (i.e., dampers) is very effective in mitigating the dynamic responses as well as minimizing the chances of pounding [4-7]. This approach takes advantage of the interaction between adjacent structures with connection to reduce the seismic responses of the structures if the control methods and device parameters are selected appropriately. Since the seismic responses and reduction effectiveness of the adjacent structures connected by dampers are closely related to the linking damper parameters as well as to the structural features, enormous efforts have been made to study the optimum connecting parameters of dampers for seismic mitigation in recent decades.

Since the seismic responses of adjacent structures linked by energy dissipation devices are more complicated than those of a monomer structure due to the vibration interaction between them, the previous seismic reduction researches were focused primarily on the two-adjacent-structure system for simplicity so far. Zhang and Xu [8, 9] performed the numerical investigations of dynamic characteristics and seismic responses of two adjacent structures linked by discrete viscoelastic dampers. They identified the optimum parameters of the Voigt and Maxwell model-defined dampers by maximizing the modal damping ratios through extensive numerical parametric studies.

All the above researches to find the optimum parameters of dampers linking two adjacent structures, however, were carried out for specific adjacent structures, and no analytical formulas for the optimum parameters of dampers were provided. From a practical point of view, it is better to provide general analytical formulas to facilitate the selection of the optimum parameters of linking dampers for seismic reduction. To this end, Zhu and Iemura [10-13] modeled two adjacent structures as two single-degree-of-freedom (SDOF) systems and derived the general analytical formulas for the optimum stiffness and damping ratio of the Voigt, Kelvin and Maxwell model-defined damper, respectively, connecting two SDOF systems subjected to a white-noise ground excitation. Based on the analysis model of two undamped adjacent SDOF structures connected by viscous damper under the harmonic excitation as well as stationary white-noise process, the closed-form expressions for optimum damping of viscous damper for minimum steady state as well as minimum mean square relative displacement and absolute acceleration of either of the connected SDOF structures are derived by Bhaskararao et el. [14]. The optimum damping of connecting damper is found to be functions of mass and frequency ratio of two connected structures. Recently, Karabork [15, 16] investigated the optimum values of viscous dampers placed between structures, which are modeled as shear frames with different height ratios, to prevent pounding under different earthquake accelerations. The influences of the adjacent multistory structures height ratios on the optimum linking parameter and corresponding seismic reduction effectiveness are studied.

To date the studies reported in the literature cited have been limited mainly to two-building connected systems. However, the multi-adjacent-building systems composed of more than two structures are more common in practical construction, such as a large-scale building comprising multiple towers and large podium separated by seismic joints from each other, or groups of structures constructed closely. Some preliminary seismic reduction researches on three adjacent structures linked by dampers were carried out. Kim et al. [17] investigated the seismic reduction effectiveness of three adjacent structures linked by viscoelastic dampers. Parametric studies were conducted using three SDOF system connected by dampers and subjected to white noise and earthquake ground excitations. Based on a three-building model connected by dampers or/and actuators, the seismic performances of the controlled systems subjected to earthquake excitations were investigated by Zou et al. [18]. Recently, Zhang et al. [19] performed a preliminary study on the energy flow in the elastic phase of a three-adjacent-structure controlled system with supplemental Kelvin-type dampers. The control effect, energy transfer and distribution of the system under uncertain and deterministic excitations are investigated. Besides the aforementioned three adjacent structures connected, the earthquake-induced pounding amongst separated three adjacent MDOF linear elastic systems was analyzed with considering the effect of soil structure interactions [20, 21].

The abovementioned studies verified the seismic reduction effectiveness of three-adjacent-structure system connected by dampers using theoretical and numerical methods. The influences of linking damper parameters as well as structural dynamic constants on the structural responses including displacement, shear force and energy distribution were compared. So far, relatively little research has been undertaken to optimize parameters of dampers connecting multi-adjacent-structure system for engineering application.

In this study, the connecting parameters optimization of Kelvin-modeled viscoelastic dampers to be placed among symmetric three adjacent structures and the corresponding seismic responses reduction effectiveness are investigated numerically. The influences of the connecting stiffness and damping values on the reduction effectiveness are researched and then the optimum linking parameters are obtained according to the three control criteria respectively. The relations between the optimum parameters and the structural characteristics parameters, i.e., the structural mass and vibration frequency ratios, are analyzed. Additionally, the applicability of the optimum parameters derived from simplified model are examined by an example system of MDOF modeled three-adjacent-structure.

2 Analysis Model and Equations of Motion

2.1 Simplified Analysis Model

The three-adjacent-structure system interconnected by Kelvin-modeled dampers is illustrated in Fig.1. The main analysis objective is to study the optimum parameters of the linking dampers, i.e., connecting stiffness and damping coefficient, for the structural seismic response mitigation. The analysis of coupled structures is inherently complex because all the structures are MDOF systems and the number of degrees of freedom of coupled system can be excessively large. Moreover, the optimal parameters obtained from a specific combined system composed of three structures of MDOF may not be applicable for other general structures. Important physical insights into complex coupled system behavior can be gained by using more simplified procedures while demanding less-detailed response information. Consequently, only a simple 3-DOF system subjected to seismic excitation, with two interaction elements, representing the three-adjacent-structure connected system, is considered here as shown in Fig.2. The three adjacent structures (referred as Structure-1, -2 and -3) are respectively specified by their first modal masses, m_1, m_2, and m_3, along with the horizontal relative displacement, x_1, x_2 and x_3; the system spring constant, k_1, k_2 and k_3; damping constant, c_1, c_2 and c_3; the connecting damper stiffness and damping coefficient, k_{01}, c_{01} and k_{02}, c_{02}; and the ground horizontal motion acceleration, $\ddot{x}_g(t)$. The damper connection between Structure-1 and -2 on the left-hand side is referred as connection-1, and that between Structure-2 and -3 on the right-hand side as connection-2.

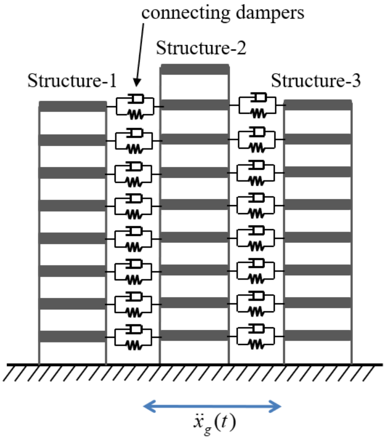

Fig. 1. Three adjacent structures linked by dampers

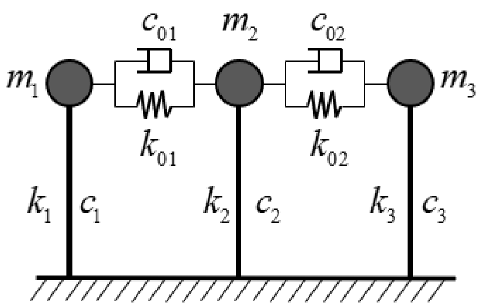

Fig. 2. Simplified model

2.2 Equations of Motion

The equation of motion of the simplified 3-DOF system subjected to earthquake excitation, shown in Fig.2, is expressed as follows:

$$M\ddot{X} + C\dot{X} + KX = -MI\ddot{x}_g(t) \tag{1}$$

where the structural mass, damping and stiffness matrices can be written for the coupled system as:
$M = \begin{bmatrix} m_1 & & \\ & m_2 & \\ & & m_3 \end{bmatrix}$, $C = \begin{bmatrix} c_1 + c_{01} & -c_{01} & 0 \\ -c_{01} & c_2 + c_{01} + c_{02} & -c_{02} \\ 0 & -c_{02} & c_3 + c_{02} \end{bmatrix}$, $K = \begin{bmatrix} k_1 + k & -k_{01} & 0 \\ -k_{01} & k_2 + k_{01} + k_{02} & -k_{02} \\ 0 & -k_{02} & k_3 + k_{02} \end{bmatrix}$; the unit column vector $I = \{1 \quad 1 \quad 1\}^T$; $X, \dot{X}$and $\ddot{X}$are the structural relative displacement, velocity and acceleration vectors, respectively, and $X = \{x_1 \quad x_2 \quad x_3\}^T$; the superscript 'T' indicates the transpose of the associated matrix.

In order to facilitate the subsequent optimization of connecting parameters, some parameters of the structural dynamic characteristics and linking dampers are defined here. Let $\omega_1 = \sqrt{k_1/m_1}, \omega_2 = \sqrt{k_2/m_2}$, and $\omega_3 = \sqrt{k_3/m_3}$ be the natural frequencies and $\xi_1 = c_1/(2m_1\omega_1)$, $\xi_2 = c_2/(2m_2\omega_2)$ and $\xi_3 = c_3/(2m_3\omega_3)$ be the damping ratios of Structure-1, -2 and -3, respectively. Similarly, it is assumed that the connection-1 and -2 have nominal frequencies of $\omega_{01} = \sqrt{k_{01}/m_2}$ and $\omega_{02} = \sqrt{k_{02}/m_2}$, respectively, for connecting stiffness analysis. Let c_{01} and c_{02} be the damping coefficients of the connection-1 and -2 dampers, respectively. The corresponding connecting-damper damping ratios are defined as $\xi_{01} = c_{01}/(2m_2\omega_2)$ and $\xi_{02} = c_{02}/(2m_2\omega_2)$, respectively.

Let $\beta_{21} = \omega_2/\omega_1$ and $\beta_{31} = \omega_3/\omega_1$ be the frequency ratios of Strucutre-2 to -1 and Structure-3 to -1, respectively. The structural mass ratios are defined as $\mu_{21} = m_2/m_1$ and $\mu_{23} = m_2/m_3$, then the mass ratio of Structure-3 to -1 is expressed as $\mu_{31} = m_3/m_1 = \mu_{21}/\mu_{23}$. The nominal frequency ratios of connection-1 and -2 to Structure-1 are defined as $\beta_{01} = \omega_{01}/\omega_1$ and $\beta_{02} = \omega_{02}/\omega_1$, respectively. Then the stiffnesses of connection-1 and -2 can be expressed in terms of β_{01} and β_{02} as $k_{01} = m_2(\beta_{01}\omega_1)^2$, $k_{02} = m_2(\beta_{02}\omega_1)^2$.

By dividing the three equilibrium equations in matrix form Eq. (1) both sides by m_1 , m_2 and m_3 , respectively, it can be rewritten in generalized form as:

$$\bar{M}\ddot{X} + \bar{C}\dot{X} + \bar{K}X = -I\ddot{x}_g(t) \tag{2}$$

where, $\bar{M} = \begin{bmatrix} 1 & & \\ & 1 & \\ & & 1 \end{bmatrix}$, $\bar{C} = \begin{bmatrix} a_1 & a_3 & 0 \\ a_5 & a_7 & a_7 \\ 0 & a_{11} & a_{13} \end{bmatrix}$, $\bar{K} = \begin{bmatrix} a_2 & a_4 & 0 \\ a_6 & a_8 & a_{10} \\ 0 & a_{12} & a_{14} \end{bmatrix}$, in which the matrix elements a_n $(n = 1,2, \dots 14)$ are the functions of the previously defined parameters.

3 Optimization Criterion

Lin et al. [22] put forward a pseudo-excitation algorithm, which provides a useful method for dynamic response analysis of complex engineering structures under random excitations. The earthquake random excitations can be converted to a series of harmonic excitations. The pseudo-excitation is constituted as follows:

$$\ddot{x}_g(t) = \sqrt{S_g(\omega)} \cdot e^{i\omega t} \tag{3}$$

where $S_g(\omega)$ is the power spectral density (PSD) of ground motion; 'i' is the imaginary unit. Then the displacement, velocity and acceleration responses of the 3-DOF system are given as [22, 23]:

$$X = H(i\omega) \cdot \sqrt{S_g(\omega)} \cdot e^{i\omega t}, \dot{X} = (i\omega)H(i\omega) \cdot \sqrt{S_g(\omega)} \cdot e^{i\omega t}, \ddot{X} = (i\omega)^2 H(i\omega) \cdot \sqrt{S_g(\omega)} \cdot e^{i\omega t} \tag{4}$$

where $H(i\omega) = \{H_1(i\omega) \quad H_2(i\omega) \quad H_3(i\omega)\}^T$, in which $H_1(i\omega)$, $H_2(i\omega)$ and $H_3(i\omega)$ are the complex frequency response functions for displacement of the three degrees of freedom, respectively; ω is the circular frequency of excitation.

Substituting Eqs. (3) and (4) into Eq. (2) yields:

$$\widehat{D} H(i\omega) = -I \tag{5}$$

where the matrix $\widehat{D} = \begin{bmatrix} d_{11} & d_{12} & 0 \\ d_{21} & d_{22} & d_{23} \\ 0 & d_{32} & d_{33} \end{bmatrix}$, in which the elements d_{ij} are the functions in terms of an. From Eq. (5) the solution of complex frequency response functions $H(i\omega)$ can be obtained. Using the functions, the PSD of velocity response is given by:

$$S_{\dot{x}_j} = \left|(i\omega)H_j(i\omega)\right|^2 \cdot S_g(\omega) \ (j = 1,2,3) \tag{6}$$

The mean square response can be expressed in terms of velocity response PSD as:

$$E\left[\dot{x}_j{}^2\right] = \sigma_{\dot{x}_j}{}^2 = \int_{-\infty}^{+\infty} \left|(i\omega)H_j(i\omega)\right|^2 \cdot S_g(\omega) d\omega \tag{7}$$

Too many different control objectives, such as the structural top displacement, the absolute acceleration, the base shear force, the maximum interstorey drift, the structural vibration energy, are used alone or in combination in damper optimization problems. This study selects the time-averaged relative vibration energy as the structural response intensity evaluation for each structure subjected to random process excitation. It can be shown that the time-averaged total relative energy of each of the adjacent structures under random ground excitation is [7]:

$$E_j = m_j \sigma_{\dot{x}_j}{}^2 = m_j \int_{-\infty}^{+\infty} \left|(i\omega)H_j(i\omega)\right|^2 \cdot S_g(\omega) d\omega \tag{8}$$

where E_j is the time-averaged total relative energy of Structure-j in the adjacent structures system. Assuming the horizontal ground acceleration as a white-noise random process with a constant PSD of $S_g(\omega) = S_0$, thus Eq. (8) can be written as:

$$E_j = m_j S_0 \int_{-\infty}^{+\infty} \left|(i\omega) H_j(i\omega)\right|^2 \cdot d\omega \tag{9}$$

In the case of independent adjacent structures without connection, the time-averaged total relative energy of uncontrolled structure under the white noise excitation is:

$$E_{0j} = m_j \pi S_0 / \left(2\xi_j \omega_{j1}\right) \tag{10}$$

where ω_{j1} and ξ_j are the structural natural vibration circular frequency and damping ratio of Structure-j, respectively.

In order to analyze the influences of connecting parameters, i.e., β_{01} , β_{02} , ξ_{01} and ξ_{02}, on the structural responses, the ratio of vibration energy of controlled structure to that of uncontrolled structure is defined as structural seismic reduction factor (SRF), which is given by:

$$R_j = E_j / E_{0j} \ (j = 1,2,3) \tag{11}$$

where R_j is the SRF of Structure-j. Furthermore, the SRF of the three-structure group is defined as:

$$R_4 = (E_1 + E_2 + E_3)/(E_{01} + E_{02} + E_{03}) \tag{12}$$

The optimum connecting parameters are those lead to minimum value of structural SRF. The SRFs are related to connecting parameters, the structural frequency-ratio, mass-ratio and damping ratio, while irrelevant to specific structural natural vibration frequency values. The lower the SRF value indicates the better reduction effectiveness. Four optimization criteria are selected in this study to minimize the SRF values of R_1 , R_2 , R_3 , and R_4, respectively. The seismic reduction effectiveness is affected by structural mass-ratio, frequency-ratio, connection nominal frequency-ratio and damping-ratio. Too many research parameters will increase the difficulties in the optimization. For simplicity, it is assumed that the Structure-1 and -3 are identical and then only symmetrical three-adjacent-structure connected system is considered preliminarily in this study. Consequently, three optimization criteria totally are considered since R_1 equals to R_3. Then it will be noted that the connecting parameters include stiffness terms β_0 (represents β_{01} and β_{02}) and damping ratio terms ξ_0 (represents ξ_{01} and ξ_{02}) for symmetrical connections.

4 Effects of Connecting Parameters on Responses

The influences of connecting parameters, i.e., β_0 and ξ_0, on structural SRFs are analyzed numerically, as well as those of structural parameters, namely frequency-ratio and mass-ratio. The structural frequency-ratio β_{21} is varied from 0.1 to 5.0 and the mass-ratio μ_{21} from 0.5 to 5.0 in the numerical analysis. The damping ratio of each structure itself is taken to be 0.05. The connecting stiffness parameter β_0 is varied from 0.01 to 2.0 and the connecting damping ratio ξ_0 from 0.01 to 1.0. The numerical range covers the optimal connecting parameters for the given β_{21} and μ_{21}.

The variations of the structural SRFs with connecting parameters β_0 and ξ_0, are illustrated in Fig.3 with the mass-ratio μ_{21} is set to be 1.2 and the frequency-ratio β_{21} is of 0.5, which means the Structure-2 is more flexural and heavier than Structure-1. It is observed that both the two connecting parameters β_0 and ξ_0, evidently affects SRF value. There exists a pair of optimum values of connecting stiffness and damping to minimize each of the SRFs. The optimum connecting parameter demand is different from each other according to the control objectives. Comparing Fig.3 with Fig.4, in which β_{21}=1.8, shows that the optimum connecting stiffness is equal to 0 for the more flexural structure, namely Structure-2 in Fig.3 and Structure-1 in Fig.4, respectively. Then viscous dampers should be adopted when the flexural structure is taken as the control objective, otherwise, the viscoelastic dampers should be utilized.

It can also be observed that the larger the difference between the structural natural vibration frequencies, the better seismic reduction effectiveness could be obtained. The structural seismic reduction effectiveness deteriorates with the structural vibration frequencies approach to each other. In particular, if β_{21}=1, there are no interactions and relative motions between adjacent two of the three structures. In this case, the capacity of dissipation energy of damper has not been exploited.

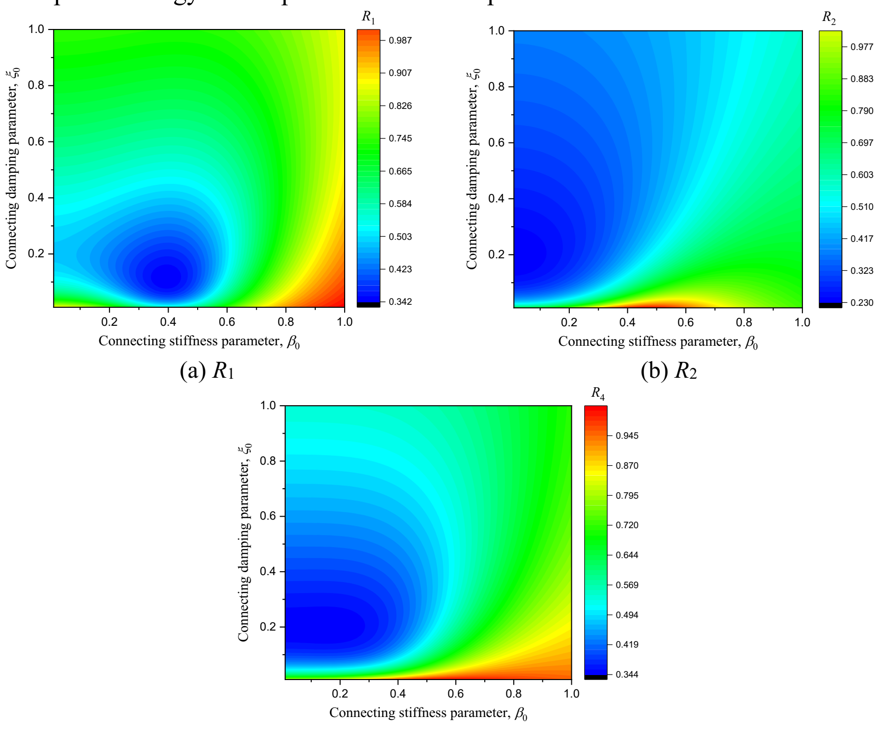

(a) R_1 (b) R_2

(c) R_4

Fig. 3. Variation of SRF with connecting parameters (μ_{21}=1.2, β_{21}=0.5)

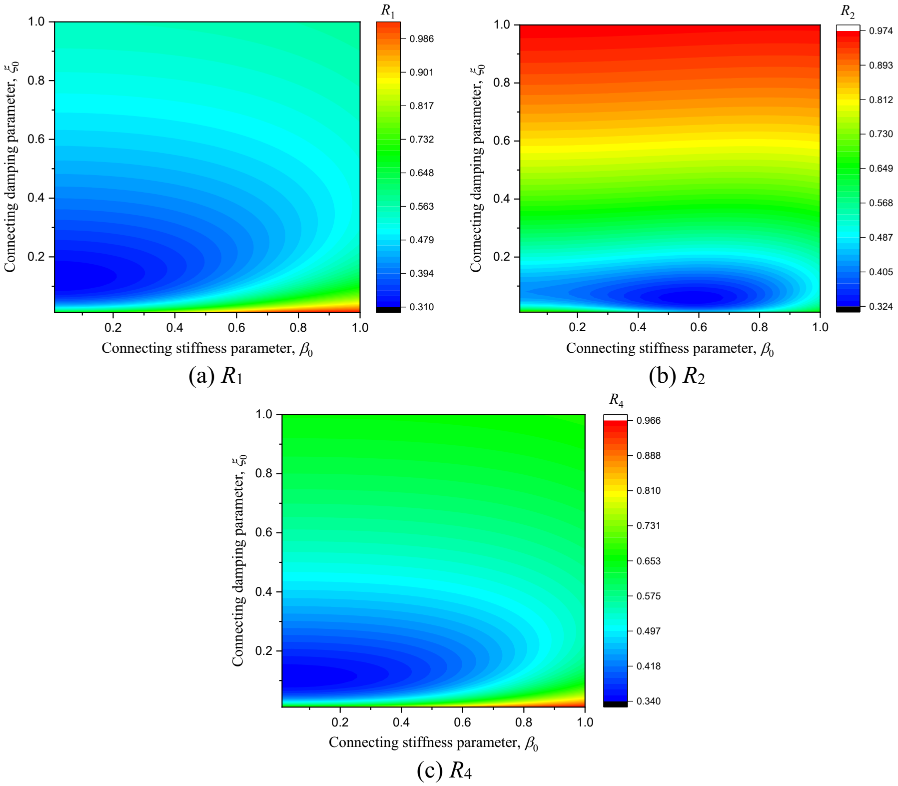

Fig. 4. Variation of SRF with connecting parameters (μ_{21}=1.2, β_{21}=1.8)

5 Optimum Connecting Parameters and Corresponding SRF

The optimum connecting parameters for each control criterion are derived through numerical analysis with each structure damping itself and the correlation between the connecting parameters considered.

5.1 Optimum Connecting Parameters for Control Criterion-I (-III)

The optimization criterion-I (-III) is to minimize the SRF value of Structure-1 (-3), herein $R_1 = R_3$ for symmetric structures system. The optimum connecting stiffness parameter β_{0opt} and damping ratio ξ_{0opt} for Structure-1 (-3) and the corresponding SRF values are portrayed graphically in Fig.5. It will be noted that when the Structure-1 is stiffer than Structure-2 (i.e., β_{21}<1), a pair of optimum connecting parameters exist for Structure-1 for the given frequency-ratio and mass-ratio. The values of optimum connecting parameters β_{0opt} and ξ_{0opt} decrease significantly with the frequency-ratio increases until to 1.0. As the mass-ratio increases, the connecting stiffness parameter

β_{0opt} decreases while the connecting damping ratio ξ_{0opt} varies slightly. On the other side, when the Structure-1 is more flexural than Structure-2 (i.e., β_{21}>1), the optimum connecting stiffness β_{0opt} equals to 0 constantly irrespective of frequency-ratio and mass-ratio variations, then the viscous dampers may be utilized in this case. The optimum connecting damping ratio ξ_{0opt} increases gradually from zero to some value with the frequency-ratio increases. The value of ξ_{0opt} decreases with the mass-ratio μ_{21}. increases. The best seismic reduction effectiveness obtained with minimum SRF value for the Structure-1, linked by dampers with optimum parameters, is plotted in Fig.5(c) for various values of structure frequency-ratio β_{21} and mass-ratio μ_{21}.. It is obviously that the larger the difference between the structural vibration frequencies, the better reduction effectiveness can be achieved. In the case that the frequencies of the structures are equal, no reduction effectiveness can be realized. The minimum SRF value decreases slightly with increasing mass-ratio μ_{21}..

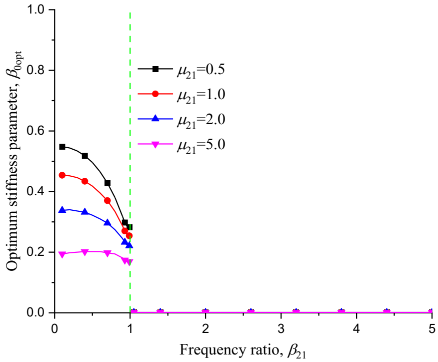

(a) Optimum connecting stiffness parameter

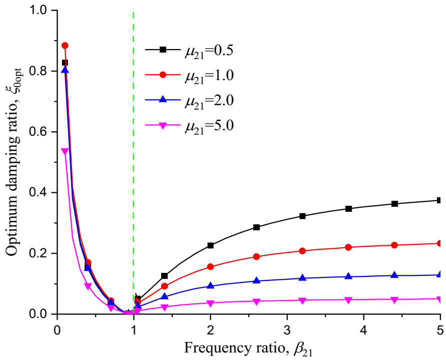

(b) Optimum connecting damping ratio

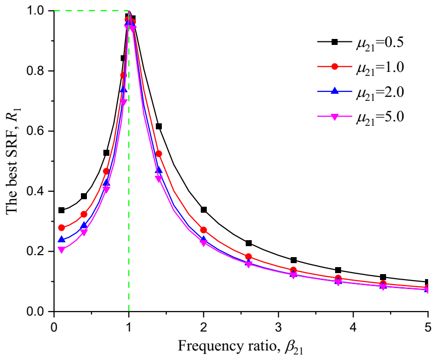

(c) Minimum SRF value of Structure-1

Fig. 5. Optimum connecting parameters and control effectiveness for control criterion-I

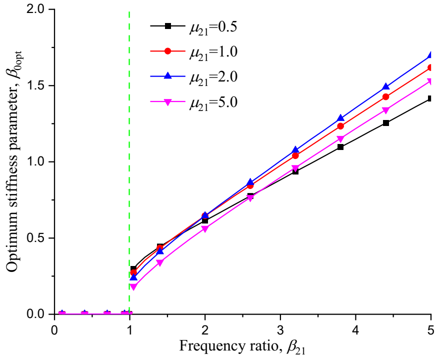

(a) Optimum connecting stiffness parameter

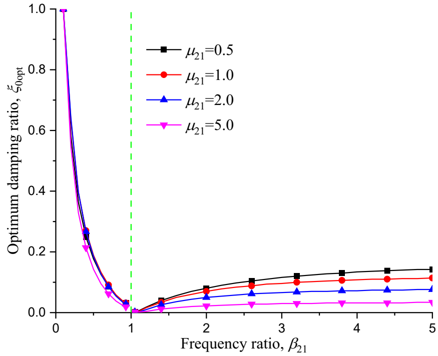

(b) Optimum connecting damping ratio

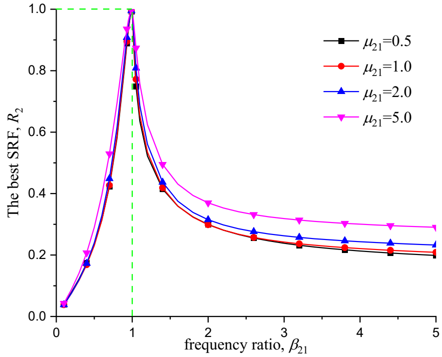

(c) Minimum SRF value of Structure-2

Fig. 6. Optimum connecting parameters and control effectiveness for control criterion-II

5.2 Optimum Connecting Parameters for Control Criterion-II

The control criterion-II takes the middle structure of the three as the control objective and the corresponding optimum linking parameters of connecting dampers and the best reduction effectiveness are indicated in Fig.6. Similarly, when the Structure-2 is the more flexural one (i.e., β_{21}<1), the optimum connecting stiffness β_{0opt} equals to 0 constantly. If the Structure-2 is the stiffer one (i.e., β_{21}>1), the optimum connecting stiffness parameter β_{0opt} increases linearly with the frequency-ratio β_{21} increases. It may be seen that the variation of the optimum connecting damping ratio for the Structure-2 with frequency-ratio and mass-ratio is similar to that for the Structure-1 by comparing Fig.6(b) with Fig.5(b). When the Structure-2 is a more flexural structure, the optimum connecting damping ratio ξ_{0opt} decreases from a large value to 0 significantly with the frequency-ratio increases in the range from 0 to 1.0. The influence of mass-ratio on the optimum parameters is slight and can be neglected. If the middle structure is a relative stiffer one, then the optimum connecting damping ratio ξ_{0opt} increases slightly from 0 to a constant with the frequency-ratio increases largely from 1.0 to 5.0. The value of optimum connecting damping ratio ξ_{0opt} decreases slightly with the mass-ratio μ_{21}. increases. It is informative to examine the seismic reduction effectiveness of the middle structure with the optimum connecting parameters by reference to Fig.6(c). It is obviously that the larger the difference between the structural vibration frequencies, the better reduction effectiveness could be obtained. The SRF value increases slightly with the mass-ratio increases.

5.3 Optimum Connecting Parameters for Control Criterion-IV

The control criterion-IV takes the whole three adjacent structures group as the control objective to minimize the SRF value of R_4 . The optimum connecting parametric pair and the best control effectiveness are shown in Fig.7. For the more flexural structure of the system, the optimum connecting stiffness parameter β_{0opt} equals to 0 constantly without variation with frequency-ratio and mass-ratio. Due to reduction factor R_4 being related to energy proportion of each structure to the total vibration energy, the optimum connecting stiffness parameter for the whole system is more complicated than that of a single structure. The variation of optimum connecting stiffness parameter β_{0opt} with frequency-ratio and mass-ratio are presented graphically in Fig.7(a). The numerical analysis finds that the optimum value β_{0opt} decreases with frequency-ratio β_{21} and mass-ratio μ_{21}. until equals to 0 when μ_{21}.>1.45 if the middle structure is the more flexural one. And on the other hand, in the case that the middle structure is the stiffer one, β_{0opt} equals to 0 when μ_{21}.≤2.70 and then increases with frequency-ratio and mass-ratio when μ_{21}.>2.70. It is similar to the control criterion-I and -II that the optimum connecting damping ratio ξ_{0opt} decreases with β_{21} when β_{21}<1 and then increases when β_{21}>1, and it decreases slightly with μ_{21}.. The best control effectiveness of criterion-IV lies between those of criterion-I and -II.

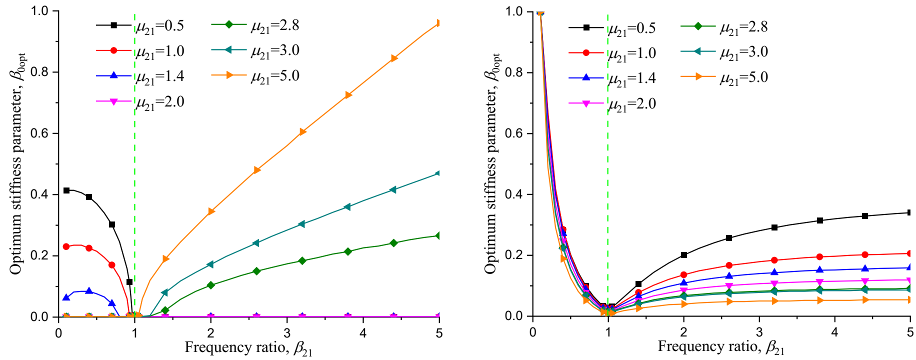

(a) Connecting stiffness parameter

(b) Connecting damping ratio

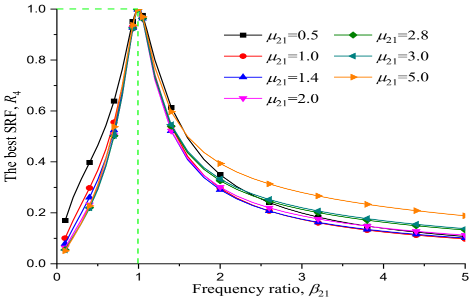

(c) The minimum SRF value of the system

Fig. 7. Optimum connecting parameters and control effectiveness for control criterion-IV

It is noted from Figs.5, 6 and 7 that the optimum connecting parameters for control criteria are not identical and then the structures could not obtain the best control effectiveness simultaneously. Fig.8 shows that the response of Structure-2 (under criterion-I) and that of Structure-1 (under criterion-II) may be magnified when the frequency-ratio β_{21} is in the range of 0.7-1.0 and of 1.0-1.25, respectively. In the other case, the responses of all structures can be suppressed to some extent when the system is connected according to the optimum parameters.

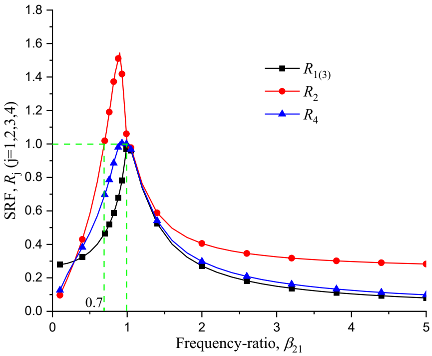

(a) SRFs under control criterion-I

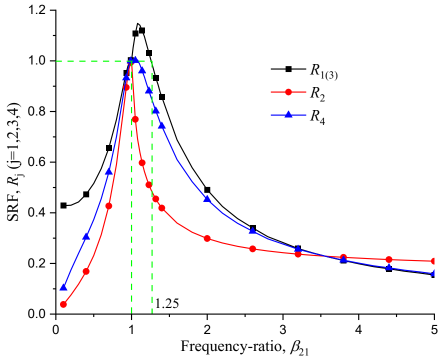

(b) SRFs under control criterion-II

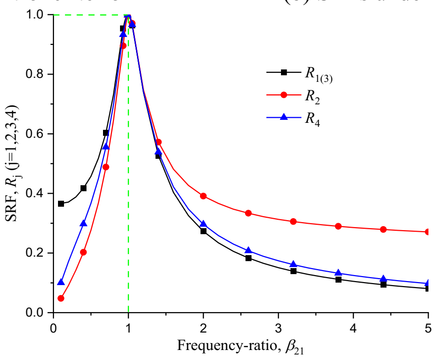

(c) SRFs under control criterion-IV

Fig. 8. Seismic reduction index under each control objective

6 MDOF Structures Connected System

The previous parts of parametric optimization and corresponding connecting parameters and control effectiveness analysis are based on the simplified model composed of three SDOF structures excited by stationary white-noise ground motion. Generally, SDOF structures are rare and nearly all structures are of multi-degree of freedom, especially for tall buildings. It is necessary to examine the applicability of the optimum parameters for MDOF structure seismic reduction.

6.1 Analysis Model and Reduction Effectiveness

Assuming a symmetric three-adjacent-structure system with the same story height is shown in Fig.1. Structure-1, -2 and -3 are constructed with n_1 , n_2 and n_3 stories, respectively, herein $n_1 = n_3 < n_2$. The dampers are connected between the two adjacent buildings at the bottom n1 stories of each structure with equal stiffness k_0 and damping coefficient c_0 to mitigate structural responses. Then the top $(n_2 - n_1)$ floors of Structure-2 are not controlled with damper.

In Eq.(1) for a 3-MDOF-structure connected system, the mass matrix $M = \begin{bmatrix} M_1 & & \\ & M_2 & \\ & & M_3 \end{bmatrix}_{(n_1+n_2+n_3)\times(n_1+n_2+n_3)}$, where M_1, M_2 and M_3 are the matrices of the three structures, respectively; the damping matrix $C = C_s + C_0$, in which the damping matrix of the structures themselves $C_s = \begin{bmatrix} C_1 & & \\ & C_2 & \\ & & C_3 \end{bmatrix}_{(n_1+n_2+n_3)\times(n_1+n_2+n_3)}$, in which the matrices C_1, C_2 and C_3 represent the damping matrix of the three structures without connecting, respectively, which are Raleigh damping modeled; the connecting damping matrix $C_0 = \begin{bmatrix} C_{11} & C_{12} & 0 \\ C_{21} & C_{22} & C_{23} \\ 0 & C_{32} & C_{33} \end{bmatrix}_{(n_1+n_2+n_3)\times(n_1+n_2+n_3)}$,

where $C_{11} = diag[C_0]_{n_1\times n_1}$, $C_{12} = [-C_{11} \quad 0]_{n_1\times n_2}$, $C_{21} = \begin{bmatrix} -C_{11} \\ 0 \end{bmatrix}_{n_2\times n_1}$,

$C_{22} = \begin{bmatrix} 2C_{11} & 0 \\ 0 & 0 \end{bmatrix}_{n_2\times n_2}$ (for symmetric system), $C_{23} = \begin{bmatrix} -C_{11} \\ 0 \end{bmatrix}_{n_2\times n_3}$, $C_{32} = [-C_{11} \quad 0]_{n_3\times n_2}$,

$C_{33} = diag[c_0]_{n_3\times n_3}$. Similarly, the stiffness matrix $K = K_s + K_0$, in which $K_s = \begin{bmatrix} K_1 & & \\ & K_2 & \\ & & K_3 \end{bmatrix}_{(n_1+n_2+n_3)\times(n_1+n_2+n_3)}$, where K_1, K_2 and K_3 represent the stiffness matrix of the three structures, respectively; the connecting stiffness matrix

$$K_0 = \begin{bmatrix} K_{11} & K_{12} & 0 \\ K_{21} & K_{22} & K_{23} \\ 0 & K_{32} & K_{33} \end{bmatrix}_{(n_1+n_2+n_3)\times(n_1+n_2+n_3)},$$

in which $K_{11} = diag[K_0]_{n_1\times n_1}$, $K_{12} = [-K_{11} \quad 0]_{n_1\times n_2}$, $K_{21} = \begin{bmatrix} -K_{11} \\ 0 \end{bmatrix}_{n_2\times n_1}$, $K_{22} = \begin{bmatrix} 2K_{11} & 0 \\ 0 & 0 \end{bmatrix}_{n_2\times n_2}$, $K_{23} = \begin{bmatrix} -K_{11} \\ 0 \end{bmatrix}_{n_2\times n_3}$, $K_{32} = [-K_{11} \quad 0]_{n_3\times n_2}$, $K_{33} = diag[k_0]_{n_3\times n_3}$.

Thus substituting these matrices, Eqs.(3) and (4) into Eq.(1) leads to the following expression:

$$[(i\omega)^2 M + (i\omega)C + K]H(i\omega) = -MI \tag{13}$$

Hence the frequency response function is found to be

$$H(i\omega) = -[(i\omega)^2 M + (i\omega)C + K]^{-1} MI \tag{14}$$

in which the superscript '-1' indicates the inverse of the associated matrix. For each structure, the total vibration energy given by Eq. (8) is rewritten as:

$$E_j = \sum_{k=1}^{n_j} m_k \int_{-\infty}^{+\infty} |(i\omega)H_k(i\omega)|^2 \cdot S_g(\omega)d\omega \tag{15}$$

The illustrative three adjacent structures are of 17-, 20- and 17-story, respectively, and connected with viscoelastic dampers between two adjacent structures among them. The story heights of all the three towers are the same, and the floor mass and interstory lateral stiffness of them are uniformly distributed vertically for each story. The floor mass is of 1.5×106 kg for all the structures and the interstory shear stiffness is 2.8×106 kN/m for Structure-1 and -3, and 2.2×106 kN/m for Structure-2. The damping ratio of each of the structures itself is assumed to be 0.05. The total vibration energy of each of the structures is the sum of the vibration energy of all the mass points of the structure. The Clough-Penzien filtered white-noise ground motion model, which has been widely used in earthquake engineering [14], is adopted in the frequency domain analysis. The characteristic parameters of the soil surrounding the structures are selected as ω_g=15.6 rad/s, ξ_g =0.6, ξ_k =0.6 and ω_k =1.5 rad/s. The intensity of ground motion S_0=4.65×10-4m^2/s^3 is chosen to represent the intensity of the earthquakes.

Through structural modal analysis, the basic natural vibration frequencies of the three structures without connection are 0.617Hz, 0.467Hz and 0.617Hz, respectively. Then the structures frequency-ratio β_{21}=0.7567 and mass-ratio μ_{21}=1.1765. Based on the former optimization analysis results, the optimum connecting parametric pair for each control objective are listed as following:

(1) criterion-I (or III): β_0=0.336, ξ_0=0.03;

(2) criterion-II: β_0=0, ξ_0=0.071;

(3) and criterion-IV: β_0=0.107, ξ_0=0.072.

The total stiffness value of the connecting dampers $K_0 = M_2(\beta_0\omega_1)^2$ and the damping constant value

$C_0 = 2M_2\omega_2\xi_0$, where the values of β_0 and ξ_0 are selected as the previous optimization results. The total values of stiffness and damping then are averagely distributed to the connections between the adjacent structures. Here there are 17 connections totally between two adjacent structures of the group. The optimum connecting stiffness and damping coefficient are listed in Table.1.

Table 1. Connecting parameters

Control criterion	Total value of connecting stiffness /(N/m)	Total value of connecting damping coefficient /(N.s^{-1}/m)	Connecting stiffness value at each connection /(N/m)	Connecting damping coefficient value at each connection /(N.s^{-1}/m)
I(III)	5.090×10^{7}	5.281×10^{6}	2.994×10^{6}	3.106×10^{5}
II	0	1.250×10^{7}	0	7.350×10^{5}
IV	5.162×10^{6}	1.267×10^{7}	3.036×10^{5}	7.450×10^{5}

The optimum connecting parameters for the MDOF system excited by filtered white-noise may be different from those derived from the previous simplified SDOF structural model excited by stationary white-noise. For the sake of convenience, the optimum connecting parameters for the MDOF model system are defined as $\bar{K}_0 = \eta_1 K_0$, $\bar{C}_0 = \eta_2 C_0$, where K_0 and C_0 are the optimum connecting stiffness and damping coefficient, respectively, from the simplified model, and η_1, η_2 are adjustment coefficients for the MDOF system. Based on the previous optimization, it is necessary to analyze the values of adjustment coefficients η_1 and η_2.

(1) Criterion-I (III) When the Structure-1 or -3 is taken as the control objective, the optimum adjustment coefficients η_1=1.17 and η_2=1.44. It is obvious that the optimum connecting parameters are different from those derived from the simplified model. The corresponding structural SRFs at the cases η_1=1.18, η_2=1.50 and η_1=1.0, η_2=1.0 are shown in Fig.9(a), from which it may be noted that the SRF values vary slightly 0.010, 0.051 and 0.028 for Structure-1 (-3), -2 and the whole adjacent structures group, respectively.

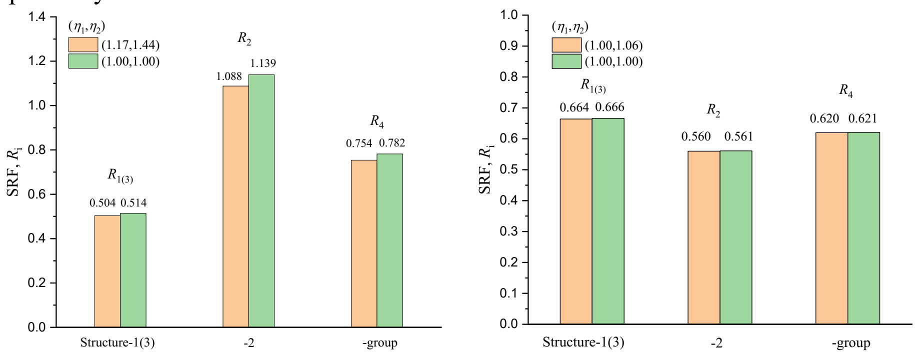

(a) Criterion-I (III) (b) Criterion-II

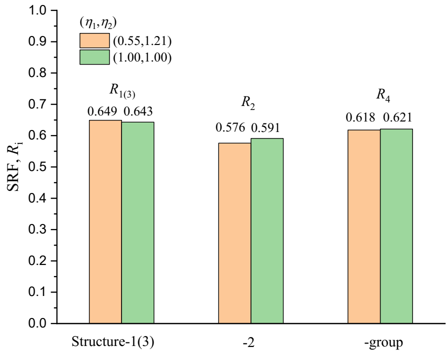

(c) Criterion-IV

Fig. 9. Variation of SRFs with adjustment coefficients

(2) Criterion-II For the middle Structure-2, its seismic reduction effectiveness reaches the best value when the adjustment coefficients η_1 and η_2 approach to 1.0 and 1.06, respectively. The corresponding SRFs are compared in Fig.9(b) when the adjustment coefficients are taken as η_1=1.0, η_2=1.06 and η_1=1.0, η_2=1.0, respectively. The variations of SRFs are only 0.002, 0.001 and 0.001 for Structure-1 (-3), -2 and the group structures, respectively.

(3) Criterion-IV For the whole three structures group, the optimum value of the adjustment coefficients are η_1=0.55 and η_2=1.21, at which the SRFs are compared with those at the values η_1=1.0 and η_2=1.0 in Fig.9(c). Correspondingly, the SRFs differences of Structure-1 (-3), -2 and the structures group are -0.006, 0.015 and 0.003, respectively.

In Fig.9, the findings demonstrate that the differences of structural seismic reduction effectiveness do not exceed 0.051 when the connecting parameters are selected according to the previous optimization results derived from the simplified model. It is obvious that the previous optimization results are applicable for MDOF systems seismic control.

6.2 Time-history Analysis under Earthquake Excitations

Since the former optimal analysis is based on the random vibration theory, the further structural time history analysis under earthquake excitation is conducted to examine additionally the applicability of the optimization results and the corresponding seismic reduction effectiveness. Due to limited space, only the adjacent three structures group, connected with dampers of optimum parameters in the case the tallest Structure-2 is taken as the control objective, is analyzed as an example. According to the current Chinese seismic design code for buildings, it is assumed that the three adjacent structures are located in the region of seismic fortification intensity (SFI) 8, design basic acceleration of ground motion 0.20g, and of the second design earthquake group. The buildings site is of category II and the characteristic period is of 0.40s. The peak ground acceleration (PGA) of earthquake waves exciting the adjacent structures is taken as 200cm/s2. There are totally 7 waves, i.e., 6 earthquake records and one artificial wave, are adopted to excite the structures.

The lateral drifts and interstory shear forces of Structure-2 under the excitations are depicted in Fig.10. By comparing the seismic responses of the controlled and uncontrolled structures, it is found that the structural displacement at the top floor is averagely decreased by 10.37% and the base shear force by 22.42%. Not only that, the top displacement and base shear force of Structure-1 (-3) are averagely mitigated by 4.15% and 11.08%, respectively. It is obvious that the seismic responses of the three structures connected with dampers are significantly reduced. Under El Centro wave excitation, the curves of earthquake input and damper dissipated energy are shown in Fig.11, which shows that the energy dissipated by connecting dampers accounts for about 42.0% of the earthquake input energy.

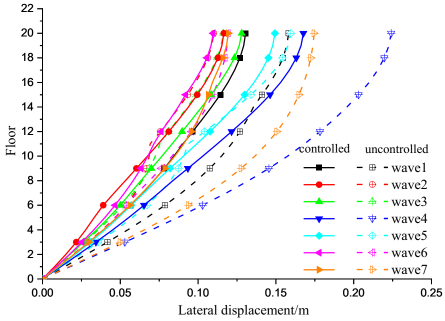

(a) Structural drift distribution

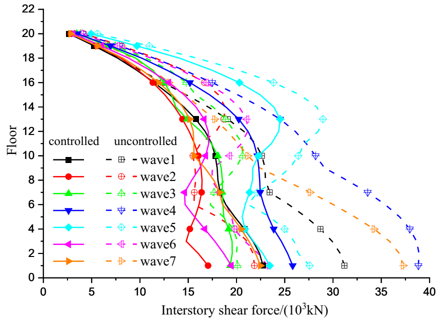

(b) Interstory shear force distribution

Fig. 10. Comparisons of structural responses

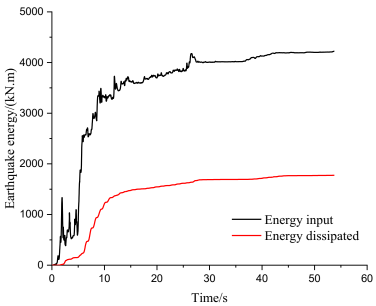

Fig. 11. Energy input and dissipated

7 Conclusions

This study investigates the effect of installing viscoelastic dampers among three adjacent structures to reduce earthquake-induced dynamic responses. The effects of connecting stiffness and damping coefficient on the seismic reduction factors of the symmetric three-adjacent-structure system are studied with numerical method. The main research conclusions are as follows:

(1) The values of connecting parameters of dampers affect the structural seismic responses significantly and the optimum connecting parameters exist for any structures

group to minimize the seismic responses. Nevertheless, the optimal connecting parametric pairs are different for each of the three structures as the control objective. For the taller and softer structure, it would be best to install viscous dampers to reduce its responses, and yet the viscoelastic dampers would be more suitable for the stiffer structure among the three adjacent ones.

(2) The lager the difference among the three adjacent structures dynamic characteristics, the better reduction effectiveness would be obtained. On the other hand, the reduction effectiveness varies slightly with the structures mass-ratio. The three adjacent structures could not reach to the best reduction effectiveness simultaneously since the optimum connecting parameters are not equal to each other for the four control criteria. When taking the more rigid structure in the three as control objective, the corresponding optimum connecting parameters for it may magnify the seismic responses of the other more flexible one adversely in a specific frequency-ratio range. Fortunately, all the structures responses could be reduced when the connecting parameters are selected according to the softer structure taken as the control objective.

(3) The derived optimum connecting parameters for three adjacent structures are related only to structures frequency-ratio and mass-ratio, not to specific structures. The optimal connecting parameters come from the simplified model are different to some extent from those derived from specific MDOF system, but the seismic reduction effectiveness of MDOF system would deteriorate slightly with SRF increases less than 0.051 when they are connected according to the proposed parameters.

Acknowledgement

This research was supported by the National Natural Science Foundation of China (Grant No. 51978389). The financial support is greatly acknowledged.

References

1. Raheem S E A, Alazrak T M A, Abdelshafy A G A, et al. (2021) Seismic pounding between adjacent buildings considering soil-structure interaction[J]. Earthquakes and Structures, 20(1):55-70. https://doi.org/ 10.12989/eas.2021.20.1.55.
2. Mohamed H, Elyamany G, Khalil E. (2021) Seismic pounding between adjacent buildings: a review. Acad Platform J. Nat Hazards Disaster Manage 2:16–28. https://doi.org/10.52114/apjhad. 937206.
3. Folhento P, De Barros RC, Braz-César M. (2021) Study on earthquake-induced structural pounding between two adjacent building structures with unequal heights. WSEAS Trans Syst 20:196–208. https://doi.org/10.37394/23202.2021.20.22.
4. Lin X F, Lin W Q. (2021) Optimal allocation and control of magnetorheological dampers for enhancing seismic performance of the adjacent structures using whale optimization algorithm[J]. Shock and Vibration, 2021: 1218956. https://doi.org/10.1155/2021/1218956
5. Elwardany H, Jankowski R, Seleemah A. (2021) Mitigating the seismic pounding of multi-story buildings in series using linear and nonlinear fluid viscous dampers. Arch Civ Mech Eng 21:137. https://doi.org/10.1007/s43452-021-00249-9.

6. Sama K J, Gur S. (2023) Optimal design of SMA damper for vibration control of connected building under random seismic excitation. Mater Today Proc. https://doi.org/10.1016/j.matpr.2023.03.554.
7. Asgarkhani N, Kazemi F, Jankowski R. (2023) Optimal retrofit strategy using viscous dampers between adjacent RC and SMRFs prone to earthquake-induced pounding. Arch Civ Mech Eng. https://doi.org/10.1007/s43452-022-00542-1.
8. Zhang W S, Xu Y L. (1999) Dynamics characteristics and seismic response of adjacent buildings linked by discrete dampers[J]. Earthquake Engineering and Structural Dynamics, 28(10):1163-1185.
https://doi.org/10.1002/(SICI)1096-9845(199910)28:10<1163::AID-EQE860>3.0.CO;2-0.
9. Zhang W S, Xu Y L. (2000) Vibration analysis of two buildings linked by Maxwell model-defined fluid dampers[J]. Journal of Sound and Vibration, 233(5):775-796. https://doi.org/10.1006/jsvi.1999.2735.
10. Zhu H P, Iemura H. (2000) A study of response control on the passive coupling element between parallel structures [J]. Structural Engineering and Mechanics, 9(4): 383-396. https://doi.org/10.12989/sem.2000.9.4.383.
11. Zhu H P, Wen Y P, Iemura H. (2001) A study on interaction control for seismic response of parallel structures[J]. Computers & Structures, 79(2): 231-242. https://doi.org/10.1016/S0045-7949(00)00119-X.
12. Zhu H P, Xu Y L. (2005) Optimum parameters of Maxwell model-defined dampers used to link adjacent structures[J]. Journal of Sound and Vibration, 279(2): 253-274. https://doi.org/10.1016/j.jsv.2003.10.035.
13. Zhu H P, Ge D D, Huang X. (2011) Optimum connecting dampers to reduce the seismic responses of parallel structures[J]. Journal of Sound and Vibration, 330(9):1931-1949. https://doi.org/10.1016/j.jsv.2010.11.016.
14. Bhaskararao A V, Jangid R S. (2007) Optimum viscous damper for connecting adjacent SDOF structures for harmonic and stationary white-noise random excitations[J]. Earthquake Engineering and Structural Dynamics, 36:563-571. https:// doi.org/10.1002/eqe.636.
15. Karabork T. (2020) Optimization damping of viscous dampers to prevent collisions between adjacent structures with unequal heights as a case study[J]. Arabian Journal for Science and Engineering, 45: 3901-3919. https:// doi.org/10.1007/s13369-019-04307-6.
16. Karabork T, Aydin E. (2019) Optimum design of viscous dampers to prevent pounding of adjacent structures[J]. Earthquakes and Structures, 16(4):437-453. https://doi.org/10.12989/eas.2019.16.4.437.
17. Kim J, Ryu J, Chung L. (2006) Seismic performance of structures connected by viscoelastic dampers[J]. Engineering Structures, 8(2):183-195.
https://doi.org/10.1016/j.engstruct.2005.05.014.
18. Zou L, Butterworth J W, Ma X. (2010) Seismic control of multi-adjacent building systems[J]. International Journal of Structural Stability and Dynamics, 10(1):21-35. https://doi.org/10.1142/S0219455410003403.
19. Zhang S R, He J M, Liu L K, et al. (2023) Energy research of three-adjacent structures connected by Kelvin-type dampers based on power flow[J]. Structures, 51:1670-1683. https://doi.org/10.1016/j.istruc.2023.03.114.
20. Pote R K, Mate N U. Structural pounding of three adjacent multi degree of freedom system under subsurface blast and seismic action by considering and ignoring the effect of soil structure interaction[C]. Materials Today: Proceedings, https://doi.org/10.1016/j.matpr.2023. 06.359.

21. Sobhi P, Far H. (2021) Impact of structural pounding on structural behaviour of adjacent buildings considering dynamic soilstructure interaction. Bull Earthq Eng 20:3515–3547. https://doi.org/10.1007/s10518-021-01195-w
22. Lin J H, Zhang W S, Li J J. (1994) Structural responses to arbitrarily coherent stationary random excitations, Computers and Structures, 50(5):629-633. https://doi.org/10.1016/0045-7949(94)90422-7
23. Ge X G, Li C D, Azim I, et al. (2021) Structural dynamic responses of linear structures subjected to Kanai-Tajimi excitation[J]. Structures, 34:3958-3967. https://doi.org/10.1016/j.istruc.2021.08.092